Thyroid

THE PRIMARY CILIUM IN THE HUMAN THYROCYTE: CHANGES IN FREQUENCY AND LENGTH IN RELATION TO THE FUNCTIONAL PATHOLOGY OF THE THYROID GLAND.

Journal:	*Thyroid*
Manuscript ID	Draft
Manuscript Type:	Clinical or Basic Original Study
Date Submitted by the Author:	n/a
Complete List of Authors:	Fernández-Santos, José María; School of Medicine. University of Seville., Citología e Histología Normal y Patológica UTRILLA, JOSÉ CARMELO; School of Medicine. University of Seville., Citología e Histología Normal y Patológica Vázquez-Román, Victoria; School of Medicine. University of Seville, Citologia e Histologia Normal y Patologica Villar-Rodríguez, José; Virgen Macarena University Hospital Gutiérrez-Avilés, Lorenzo; School of Medicine. University of Seville, Citología e Histología Normal y Patológica MARTÍN-LACAVE, INÉS; School of Medicine. University of Seville, Citología e Histología Normal y Patológica
Keyword:	Graves- Disease, Pathology-Thyroid, Thyroid Cell Biology
Manuscript Keywords (Search Terms):	ciliogenesis, primary cilia, thyrocytes, nodular hyperplasia, Grave's disease
Abstract:	Background: Primary cilia (PC) are conserved structures in the adult thyroid gland of different mammals. We have recently described that, in humans, PC are usually present as a single copy per follicular cell emerging from the follicular cell apex into the follicular lumen. Methods: To better understand the role developed by PC in thyroid hormonogenesis, we investigated their changes in different human functional thyroid diseases (diffuse toxic hyperplasia/ Grave's disease and nodular hyperplasia/nodular goiter), in comparison with normal thyroid tissue, using immunofluorescence, morphometry and electron microscopy analyzes. Results: We found significantly decreased ciliary frequencies in both nodular hyperplasia (51.16±11.69%) and Grave's disease (44.43±23.70%) vs. normal thyroid glands (76.09±7.31%). Similarly, PC lengths were also significantly decreased in both nodular hyperplasia (2.02±0.35 µm) and Grave's disease (2.42±0.48 µm) compared to normal glands (3.93±0.90 µm). Moreover, in Grave's disease patients, hyperactive-follicle foci always showed diminished ciliary frequency and length compared to any other thyroid follicle pattern, independent of their thyroid status. Conclusions: Our results suggest a direct relationship between ciliogenesis and both follicle activity and tissue heterogeneity. Furthermore, the

	analysis of PC patterns in the "normal-appearance areas" of Grave's disease thyroid samples could be useful to identify subgroups of patients, who would be expected to have a poorer response to antithyroid drug treatment.

THE PRIMARY CILIUM IN THE HUMAN THYROCYTE: CHANGES IN FREQUENCY AND LENGTH IN RELATION TO THE FUNCTIONAL PATHOLOGY OF THE THYROID GLAND.

Fernández-Santos JM[1]*, Utrilla JC[1]*, Vázquez-Román V[1]*, Villar-Rodríguez JL[2], Gutiérrez-Avilés L, and Martín-Lacave I[1].

University of Seville, School of Medicine, Department of Normal and Pathological Cytology and Histology, Seville, Spain.

Department of Pathology of "Virgen Macarena" University Hospital, Seville, Spain.

*These authors have contributed equally to this work.

Corresponding author:

Prof. Inés Martín-Lacave

University of Seville, School of Medicine, Department of Normal and Pathological Cytology and Histology. Av. Sánchez Pizjuán S/N. 41009, Seville, Spain.

Phone: +34954551797

Fax: +34954551799

Email: ilacave@us.es

Fernández-Santos JM: jmsantos@us.es

Utrilla JC: utrilla@us.es

Vázquez-Román V: mvazquez2@us.es

Villar-Rodríguez JL: jlvillar@us.es

Gutiérrez-Avilés L: loguav@gmail.com

Martín-Lacave I: ilacave@us.es

Running Title: Primary cilia in human thyrocytes

Key Words: ciliogenesis, primary cilia, thyrocytes, nodular hyperplasia, Grave's disease

ABSTRACT

Background: Primary cilia (PC) are conserved structures in the adult thyroid gland of different mammals. We have recently described that, in humans, PC are usually present as a single copy per follicular cell emerging from the follicular cell apex into the follicular lumen. **Methods:** To better understand the role developed by PC in thyroid hormonogenesis, we investigated their changes in different human functional thyroid diseases (diffuse toxic hyperplasia/ Grave's disease and nodular hyperplasia/nodular goiter), in comparison with normal thyroid tissue, using immunofluorescence, morphometry and electron microscopy analyzes.

Results: We found significantly decreased ciliary frequencies in both nodular hyperplasia (51.16±11.69%) and Grave's disease (44.43±23.70%) *vs*. normal thyroid glands (76.09±7.31%). Similarly, PC lengths were also significantly decreased in both nodular hyperplasia (2.02±0.35 µm) and Grave's disease (2.42±0.48 µm) compared to normal glands (3.93±0.90 µm). Moreover, in Grave's disease patients, hyperactive-follicle foci always showed diminished ciliary frequency and length compared to any other thyroid follicle pattern, independent of their thyroid status.

Conclusions: Our results suggest a direct relationship between ciliogenesis and both follicle activity and tissue heterogeneity. Furthermore, the analysis of PC patterns in the "normal-appearance areas" of Grave's disease thyroid samples could be useful to identify subgroups of patients, who would be expected to have a poorer response to antithyroid drug treatment.

INTRODUCTION

Since their discovery by Zimmermann in 1898, primary cilia (PC) have been found in the vast majority of cell types in vertebrates, such as renal tubule (1), bile duct (2, 3), pancreatic cells (4), neurons (5, 6), keratinocytes, fibroblasts, endothelial (7) and thyroid cells (8-12). In the last decade, PC have emerged as key organelles in numerous cellular, physiological and developmental processes (13-15). In most models, PC act as extracellular sensory antennae associated with several important signalling pathways, e.g., Wnt (wingless-Int-1), PCP (planar cell polarity) and Hedgehog pathways (16-18). Alterations in PC structure or function have been reported to be responsible for several human diseases, so-called ciliopathies (19-21).

Primary ciliogenesis is inversely correlated with cell cycle progression, and PC have been proposed as negative regulators of cell division. PC are disassembled at late S phase of the cell cycle and are considered organelle characteristics of cells in a differentiated state (22, 23). Moreover, primary ciliogenesis requires an established apical membrane domain and shares several protein complexes also necessary for cell polarization and apical delivery (24, 25).

We have recently described that PC are conserved structures in the adult thyroid gland of different mammals (human, pig, guinea pig and rabbit), where they are usually present as a single copy per follicular cell (12). We have also demonstrated the presence of PC in commonly normal (Nthy-ori 3-1) and neoplastic (FTC-133 and 8505C) human thyroid cell lines, and reported that their frequency was lower in neoplastic compared to normal thyroid cells. In addition, defects in ciliogenesis have been described in malignant thyroid diseases, including papillary thyroid carcinoma and Hürthle carcinoma (26).

The thyroid gland is unique endocrine organ composed of follicles with the thyrocytes organized as an apicobasal-polarized epithelium surrounding a lumen, in which their secretory product - thyroglobulin - is stored extracellularly in large quantities. Thyroid follicles are considered the morphological and functional units of the gland, which are subjected to independent self-regulatory mechanisms that would be responsible for the heterogeneous nature of thyroid tissue (27-30). In fact, in normal thyroid tissue, smaller active follicles displaying high columnar polarized epithelium coexist with larger hypofunctioning follicles surrounded by low cuboidal or

flattened thyrocytes; this -size and activity- tissue heterogeneity are a hallmark of the human normal thyroid gland (31).

It is plausible to assume that in thyrocytes, PC, taking advantage of their ideal localization extending from the follicular cell apex into the follicular lumen, sense the colloid environment, and this sensory activity coupled to specific intracellular downstream signalling pathways contributes to the complex mechanism of thyroid hormones synthesis. Consequently, defects in ciliogenesis should be present in functional thyroid diseases such as diffuse toxic hyperplasia (Grave's disease) or nodular hyperplasia (nodular goiter), which are characterized by hormone biosynthetic deregulation, changes in follicle integrity, and altered proliferation rate.

Specifically, Grave's disease thyroid samples, from patients subjected to prior treatment with antithyroid drugs, show a highly marked variability from area to area, ranging from diffuse hyperplasia exhibiting tall columnar thyrocytes, papillary infoldings and very little light stained colloid to zones displaying different degrees of regression of the hyperfunctioning changes characterized by flat cells and increased colloid stores (32, 33). Nodular hyperplastic thyroid tissue also shows follicles that exhibit high heterogeneity in size and morphology, varying from small follicles with minimal amounts of colloid lined by high columnar thyrocytes, to very large follicles containing abundant colloid lined by flat epithelium; these large follicles are considered the characteristic pattern of nodular hyperplasia (34-36).

Although PC are key organelles that have been associated with an increasing number of pathologies and whose presence in the surface of the thyrocyte has been known for decades (9-12), there is a complete lack of information in the literature regarding the putative role that they could play in either the normal thyroid or in functional thyroid disease.

To better understand the role developed by PC in thyroid hormonogenesis, in the present study, we investigate the changes they exhibit in the normal human thyroid gland and in different functional thyroid diseases, using both morphometrical and electron microscopy analysis. Interestingly, we found significant differences in ciliary frequency and length in both nodular hyperplasia and Grave's disease compared to normal thyroid tissue. In the context of thyroid tissue heterogeneity, changes in ciliogenesis were also demonstrated in relation to the different histological patterns exhibited by thyroid follicles in Grave's disease. Finally, when low ciliary frequencies and axonemal lengths were noticeable in the apparently normal areas trapped in GD

thyroid samples, a poorer response to antithyroid drug treatment was observed The identification of the molecular mechanisms underlying defective ciliogenesis in thyroid pathology could help to understand the role played by PC in thyroid hormone biosynthetic activity and could shed light on the histopathological features of thyroid functional diseases.

MATERIAL AND METHODS

Human thyroid specimens

Five human thyroid samples -three obtained from families with hereditary medullary thyroid carcinoma who underwent a prophylactic thyroidectomy, and two normal samples adjacent to resected papillary thyroid carcinomas- were used as normal thyroid glands (NT). Ten nodular hyperplasia (NH) or multinodular goiter, and 10 diffuse toxic hyperplasia or Grave's disease (GD), were obtained from patients undergoing thyroid surgery, diagnosed at the Department of Pathology of the Virgen Macarena University Hospital of Seville. Tissue samples were collected in agreement with approval from the Research Ethics Committee of the Virgen Macarena University Hospital (C.P.-C.I. 1921). The clinicopathologic features of the patients are summarized in Table 1.

Thyroid glands were fixed in 10% neutral buffered formalin, embedded in paraffin by standard procedure, sectioned at 4-5 µm thickness, and mounted on silane-coated glass slides. Consecutive tissue sections were stained with haematoxylin-eosin for histological diagnosis and to select thyroid tissue with a characteristic appearance to perform immunofluorescence (IF).

Ultrastructural studies

Samples for transmission (TEM) and scanning (SEM) electron microscopy were obtained from the same 2 previous patients with normal-appearing thyroid adjacent to thyroid carcinoma, and from 3 and 5 of the previous patients with NH and GD, respectively.

For the TEM studies, pieces were fixed in 2.5% glutaraldehyde in 0.1M cacodylate buffer (pH 7.2), post-fixed in 1% osmium tetroxide, dehydrated in acetone and embedded in Spurr, as we have previously reported (Utrilla et al, 2015). Ultrathin sections were photographed with a Zeiss Libra 120 transmission electron microscope.

Similarly, for the SEM studies, the samples were fixed in the same glutaraldehyde solution for a minimum of 5 days and post-fixed in 1% osmium tetroxide. After dehydration, specimens were dried with the critical point method using CO_2, sputter coated with vacuum-evaporated gold, and photographed with a Zeiss EVO scanning electron microscope, as we have previously reported (12).

Double immunofluorescence staining

The double IF staining was carried out according to the same procedure that we have previously reported (12). In brief, the sections were dewaxed in xylene and hydrated through graded alcohols. An antigen retrieval step using EnVision Flex Target Retrieval Solution High pH (DM828; Dako, Denmark) was performed in a heating instrument, PTLink (Dako, Denmark). After applying washing solution, and after nonspecific blocking with 10% normal donkey serum, the primary antibody, a monoclonal anti-acetylated α-tubulin (Sigma-Aldrich, Germany), that labels the axoneme was applied. The slides were then incubated with Cy3-labeled donkey anti-mouse IgG secondary antibody (Jackson ImmunoResearch Laboratories, UK). After washing, the slides were incubated with polyclonal rabbit anti-E-cadherin antibody (Santa Cruz Biotechnology, USA) and, subsequently, with Cy2-labelled donkey anti-rabbit IgG antibody (Jackson ImmunoResearch Laboratories, UK). DAPI was added for nuclei counterstaining, and the slides were coverslipped with Dako Fluorescent Mounting Medium (S3023). Different controls for specificity of the IF technique were performed.

The samples were observed under a fluorescence microscope (Olympus BX50) equipped with a scientific digital camera (Hamamatsu ORCA-03G). All image files were processed using the Image-Pro-Plus 7.0 version software (Media Cybernetics, Rockville, USA) to create composite RGB micrographs, enhance contrast, and obtain measurements.

Morphometrical analysis

1. Analysis of primary cilia frequency

To evaluate the frequency of PC in the different functional thyroid groups, 10-20 micrographs per case at 200x magnification were morphometrically assessed using a software processing and image analysis (Cell* Imaging Software). Firstly, in every photograph, a ranking of the thyroid follicles according to their histological appearance and their size (internal perimeter) was established: (1) rounded follicles of different sizes: small-sized follicles (<50 μm), medium-sized follicles (50-100 μm),

large-sized follicles (100-500 µm) and giant follicles (>500 µm, with abundant colloid); (2) follicles with papillary infoldings; and (3) hyperfunctioning follicles, which exhibited a tall follicular epithelium and scanty colloid. The average thyroid follicles examined per patient was as follows: in the NT group, a minimum of 35 follicles per thyroid section (15 small-sized follicles, 15 medium-sized follicles, and at least, 5 large-sized follicles) were assessed; in the NH group, a minimum of 50 follicles of different sizes per section was examined, including giant follicles; and, finally, in the GD group, in which the heterogeneity among follicles was exacerbated, a minimum of 60 follicles of every pattern per gland was analyzed. Second, the frequency of ciliated vs. non-ciliated follicular cells was assessed by analysing the relative number of cilia protruding from the apical surface of the epithelium vs. the number of nuclei in adequately oriented sections of those thyroid follicles. In total, the presence of PC in the current study was evaluated in 1,300 thyroid follicles and 43,000 thyrocytes: 5,000 thyrocytes (an average of 1,000 per case) from NT glands, 18,000 thyrocytes (an average of 1,800 per case) from NH samples and, finally, 20,000 thyrocytes (an average of 2,000 per case) from GD samples.

2.- Analysis of primary cilia length

PC lengths were morphometrically assessed in 150 composite micrographs acquired using the Image-Pro-Plus 7.0 software with a 40x, UPlanFl N.A.=0.75 objective. To minimize oblique sectioned cilia length underestimation, we measured PC that were clearly well oriented towards the colloid and seemingly fully included within the 5-µm paraffin section. In brief, the length of PC was evaluated in at least 100 follicular cells per case, with a total of 2,727 cilia being measured, which corresponded to the different histological patterns established in the different groups.

Statistical analysis

Statistical differences among the percentage of ciliated thyrocytes and cilia length in different kinds of thyroid follicles of each group were measured and expressed in arbitrary units as mean ± SD. In addition, the same procedure was applied to study differences between NH, and GD, vs. NT. The data were tested by one-way ANOVA or the Student's test following the corresponding post hoc test. P values less than 0.05 were accepted as significant.

RESULTS

Histological aspects

As the existence of a correlation between follicular size and functional activity is generally accepted (with smaller follicular sizes considered more active, and the largest follicular sizes, lined by flattened cells, considered hypofunctioning follicles), in the present study, a ranking of thyroid follicles according to their size and appearance was established. In the NT group, a mixture of normal-rounded follicles of different sizes was observed, with small- and medium-sized follicles having more abundance than large follicles (Fig. 1A). In the NH group, however, follicles exhibited conspicuous differences in size, ranging from small with minimal colloid to very large colloid lakes, the so-called “giant follicles”, which were typically lined by flattened epithelium (Fig. 1B). Furthermore, in some cases of NH, Sanderson polsters’ (rounded clusters of small follicles protruding into the wall of a large follicle) appeared, together with a considerable increase in the connective tissue among follicles. Finally, in the GD group, as all patients received some form of therapy before resection, the heterogeneity in follicular pattern was paradigmatic (Fig. 1C). In addition to normal-rounded follicles of different sizes, abundant areas with hyperplastic papillae and focal areas with hyperfunctioning follicles appeared, adding to the variable presence of lymphocytic infiltrate and follicles in apoptosis (Fig. 1). As expected, no PC were identifiable in thyroid sections stained by haematoxylin and eosin.

Primary cilia detection by immunofluorescence

The presence of PC was detected in the different thyroid sections by using acetylated α-tubulin antibody and Cy3 labelling, which marked the axoneme in red. To confirm their location and frequency, E-cadherin antibody and Cy2 label were used, which marked the epithelial cell perimeter in green. Generally, PC emerged from the apical surface of thyrocytes and entered into the colloid perpendicularly.

In NT glands, all thyroid follicles exhibit ciliated cells. When the same material was analyzed at higher magnification, almost every follicular cell harboured a unique PC, although there were some cells that showed two cilia or, even more rarely, a larger number of PC (Fig. 2). In tangential sections of the thyroid follicles the PC was seen to mainly emerge from the central area of the apical surface of every thyrocyte.

In NH, the number of ciliated follicles decreased; however, at higher magnification, numerous ciliated thyrocytes were observed, although the average PC length considerably decreased (Fig. 3). In contrast, in GD, the apparent frequency of

ciliated cells varied considerably among follicles, in accordance with the enormous follicular heterogeneity inherent to diffuse toxic hyperplasia (Fig. 4). Consequently, a rigorous morphometrical study was performed to objectively evaluate the frequency of ciliated thyrocytes amongst the different functional thyroid groups.

Morphometrical analysis of primary cilia frequency

In NT glands, 76.09±7.31% of the thyrocytes were ciliated, with non-statistically significant differences among follicles of different sizes (Fig. 5A).

In thyroid sections of NH, the percentage of ciliated cells decreased up to 51.16±11.69%, with non-statistically significant differences among follicles of different sizes (Fig. 5B). When these data were compared with those found in NT glands, very significant difference appeared ($p<0.001$) (Fig. 6).

In sections of GD, the percentage of ciliated cells decreased even further up to 44.43±23.70%, with the high standard deviation a consequence of the variety of follicular patterns assessed (Fig. 5C). This value was statistically significant in comparison to that of NT ($p<0.001$) (Fig. 6). In relation to intra-group differences in the percentage of ciliated thyrocytes among the various histological patterns characteristics of GD, no significant differences were found between rounded follicles of different sizes (49,71.0±4.60%) and papillary follicles (45.31±19.89%), however, a significant difference was found when those patterns were compared with hyperfunctioning follicles (16.01±4.86%) ($p<0.001$) (Fig. 5C).

Furthermore, in GD, the percentage of ciliated thyrocytes in “normal rounded-follicle areas” was markedly different among cases, in correspondence with the subsistence of signs of thyroid biosynthetic hyperactivity after long-term antithyroid drug treatment. Thus, primary cilia frequency in those “normal areas” was significantly lower in patients who exhibited either remaining hyperactive follicle foci, high T_4 serum levels, or both compared to those patients who became euthyroid after carbimazole treatment (Fig. 7).

Analysis of primary cilia length

The length of PC showed characteristics alterations according to the pathological functional state of the thyroid gland (Fig. 8). Specifically, in NT glands, the normal thyrocytes showed the longest PC, with an average length of 3.93±0.90 µm. In contrast, thyrocytes in NH exhibited the shortest PC, with an average length of 2.02±0.35 µm, and the data were very statistically significant in comparison with the controls ($p<0.001$). Finally, in GD, the average length of PC reaches a value of

2.42±0.48 µm, which was very significant when compared to NT ($p<0.001$) and to NH ($p<0.001$). In all groups, no intra-group differences among follicles of different sizes were established. Nevertheless, it is necessary to specify that in the GD group, as hyperfunctioning follicles scarcely possess PC, most PC in this group were measured in the rest of the thyroid follicles, implying a favourable bias in the final length of the PC, which would mean that the true length could be even lower.

Finally, and similar to what is described above for primary cilia frequency, axonema lengths were also significantly lower in the "normal areas" adjacent to hyperactive follicle foci in those GD cases that showed hyperfunctioning signs, high T_4 serum levels, or both compared to those patients showing no sign of hyperactivity after antithyroid treatment (Fig. 9).

Ultrastructure of primary cilia

TEM analysis of specimens of NT glands revealed a sporadic presence of PC, located on the apical surface of follicular cells protruding into the colloid (Fig. 10). Usually only one PC per cell was present although occasionally two-three cilia together were observed. Proximally, the cilium ended in a typical basal body, in whose proximity a centriole was observed (Fig. 10A2). When NT samples were observed by SEM, follicular cells showed a polyhedral outline with 4 to 7 sides. The cell surfaces, which were generally convex, presented numerous microvilli and, emerging among them from the geometric center of the thyrocyte, one PC protruding into the colloid (Fig. 11A).

In NH thyroid glands, more sporadic PC than in controls were observed by TEM, likely as a consequence of the larger size of most thyroid follicles (Fig. 8B). The differences in follicular size were striking when observed by SEM (Fig. 11B). However, PC were easily distinguished, preferably in medium-size follicles, although they tended to disappear when the thyrocytes acquired a squamous-like appearance or when they displayed a very convex apical surface (Fig 11. B3).

In GD, the concurrent use of TEM and SEM confirmed the extreme heterogeneity among follicles. There were astounding images of follicles bearing papillae or complex mosaics of follicular surfaces with variable amounts of microvilli cilia (Fig. 10C). Despise that complexity, PC could be observed emerging among microvilli, sporadically by TEM, and frequently by SEM, although at less magnitude than in NT glands (Fig 11. C).

DISCUSSION

In the present manuscript, we show differences in the frequency, distribution and morphology of PC in human thyroid functional pathology compared to normal thyroid glands. Both GD and NH showed lower frequency of ciliated thyrocytes and shorter axonemal lengths when tissue samples were analyzed as a whole and when compared to the control group. Moreover, in the context of the pronounced tissue heterogeneity characteristic of normal thyroid itself and, particularly, of functional thyroid pathology, the different follicular patterns also exhibited changes in ciliogenesis, with a generally lower frequency of ciliated thyrocytes in zones with altered follicles compared to those areas where normal-appearance follicles predominate, with PC almost absent in hyperfunctioning areas of GD. Finally, when low ciliary frequencies and axonemal lengths were noticeable in the apparently normal areas trapped in GD thyroid samples, a poorer response to antithyroid drug treatment was observed.

In contrast to motile cilia, PC are rarely described in the evaluation of pathology specimens because PC are not readily identifiable with standard stains such as haematoxylin and eosin. Therefore, the first report in which the presence of PC was analyzed in thyroid pathology by using alternative methods, such as SEM and TEM, was not published until 1987, by Nesland et al (37). These authors qualitatively appreciated that almost every follicular cell possessed PC in the normal thyroid as well as in most goiters, but PC occurred less frequently in GD. Additionally, PC became gradually reduced from normal glands, through adenomas, well-differentiated thyroid carcinomas to anaplastic carcinomas (37). Later, we reported the presence of PC in the thyroid gland of different mammals, as well as in different human thyroid cell lines, using both double IF and electron microscopy (12). The use of IF to identify PC afforded us to analyze more extensive areas from paraffin-embedded thyroid samples, added to the additional advantage of applying quantitative methods to objectively assess changes in PC frequency and length, as was later done by Lee et al. (26), who studied the distribution of PC in different thyroid pathology and cell lines. Specifically, they described decreased frequencies of ciliated follicular cells in Hürthle thyroid carcinoma and the oncocytic variant of papillary thyroid carcinoma but reported no differences in ciliogenesis in the conventional variant of papillary thyroid carcinoma, follicular carcinoma, Hashimoto's

thyroiditis and benign nodular hyperplasia, when compared to normal thyroid tissue. In the present paper, however, after evaluating more than 1,300 thyroid follicles and 43,000 thyrocytes, we show a high degree of intra-case and inter-cases variability in the frequency and length of PC in functional thyroid pathology.

Thyroid follicles together with their adjacent capillaries form the so-called "angiofollicular units" (AFUs) that are considered the functional and morphological units of the thyroid gland (27-30). In AFUs, the enzymatic machinery for Tg iodination -named thyroxisome- is located and restricted at the apical plasma membrane of thyrocytes (38, 39). These cells constantly produce moderate amounts of H_2O_2 and other potentially toxic ROS that are physiologically required for thyroid hormone synthesis and are finely regulated (40, 41). When the synthesis process is altered, oxidation reactions start to occur in the cytoplasm with devastating consequences, such as morphological and functional breakdown, which engender disease processes, including those of autoimmune or neoplastic nature (29, 38, 42-44).

As previously shown, thyroid PC are harboured at the apical surface of almost every thyrocyte protruding into the follicular lumen (12). Taking advantage of its ideal localization, the ciliary membrane might possess specific receptors that could sense, in some specific way, either the level of iodinated thyroglobulin stored in the colloid or the thyroid oxidative charge associated with the outer surface of the plasma membrane, such as the presence of iodinated or peroxidized phospholipids that are presumed to be toxic (38). These sensory activities would be coupled in coordination with the biosynthetic process through specific intracellular downstream signalling pathways.

According to Colin et al. (42), another interesting aspect to be considered is the fact that, besides size and epithelium morphology, hyperfunctioning and hypofunctioning follicles differ in the presence and/or the amount of dense colloid-containing globules of thyroglobulin. Under increased TSH stimulation, this compact form of colloid, present in resting hypofunctioning AFUs, can be fragmented and metabolized into soluble thyroglobulin molecules to synthesize thyroid hormones (45-48). As we previously discussed (12), it would also be reasonable to hypothesize that, in thyroid follicles, PC might act as mechanosensors for the refilling of the follicular lumen with thyroglobulin to form the colloid. Thus, alterations in ciliogenesis could be related to differences in the activity of AFUs.

In accordance with what is stated above, defective ciliogenesis might be associated with failure in many processes of thyrocyte function, such as loss of apicobasal polarization of the follicular epithelium, increased intrafollicular oxidative stress, hyperstimulation or increased proliferation rate, depending on the different outcomes of thyroid disease and on the genetic or biochemical background of the patient. Specifically, in our study, despite the marked heterogeneity inherent to thyroid tissue, no ciliary differences among different patterns of thyroid follicles were observed in either NT or NH, not even in the inactive giant follicles characteristic of NH. However, in GD, hyperactive follicles foci always showed altered cilia frequency and length compared to any other thyroid follicle pattern, independent of other clinical parameters, suggesting a direct relationship between ciliogenesis and both: follicle activity and thyroid tissue heterogeneity. In this context of thyroid heterogeneity, we observed that when even the “normal-appearance areas” of GD thyroid samples showed decreased ciliogenesis, it was accompanied by signs of residual thyroid hyperactivity and worse treatment response. These findings, if confirmed by further research, would be useful to improve the therapeutic strategies for identifying subgroups of GD patients who would be expected to have a poorer response to antithyroid drug therapy.

Hassounah et al. (49), in prostatic tumorigenesis, reported that PC frequencies and lengths in the “normal tissue” surrounding prostate cancer correlated with many clinical outcomes, including size, stage and risk of recurrence suggesting the possibility of a “field effect” of PC pattern as an early event in prostate tumorigenesis.

According to Ergin et al. (50), incidental micro-papillary thyroid carcinoma (MPTC) is found in 28% of EG and 26% of NH patients; GD patients with MPTC were significantly younger, and the incidence of MPTC was additionally higher in GD patients with higher TSH levels (51). Similar to that described by Hassounah et al. (49) for prostatic cancer, the ciliary loss we describe in the present study in GD and NH thyroid tissue, could be involved in the high frequency of MPTC found in these patients. Accordingly, it would be reasonable to hypothesize a “field effect” for decreased ciliogenesis that would precede neoplastic transformation of GD or NH thyroid tissue. The possibility of these patients having an increased risk to develop an incidental MPTC would also be interesting to be explored by further research.

In conclusion, in the present study, we show that differences in thyroid primary ciliogenesis are associated with functional pathology and, moreover, with thyroid tissue heterogeneity. Our observations suggest that the contribution of PC to thyroid function, including their role in the complex mechanism of hormone synthesis, in the self-regulation of the AFUs and, eventually, in the origin of functional and neoplastic disease is an attractive hypothesis that requires further investigation.

ACKNOWLEDGMENTS

This work was supported by grants from the Consejería de Innovación, Ciencia y Empresa (refs. CTS-439/2017). The authors thank Mr. John Brown for the corrections of the English language, Mr. Marcos Ortega for histological sample processing and the Microscopy Service of CITIUS (General Research Services, Seville University, Spain) for technical assistance with electron microscopy studies.

DISCLOSURE STATEMENT

No competing financial interests exist.

REFERENCES

1. Flood PR, Totland GK 1977 Substructure of solitary cilia in mouse kidney. Cell Tissue Res. **183**:281-290.

2. De La Iglesia FA, Porta EA 1967 Ciliated biliary epithelial cells in the livers of non-human primates. Experientia. **23**:49-51.

3. Huang BQ, Masyuk TV, Muff MA, et al. 2006 Isolation and characterization of cholangiocyte primary cilia. Am J Physiol Gastrointest Liver Physiol. **291**:G500-509.

4. Aughsteen AA 2001 The ultrastructure of primary cilia in the endocrine and excretory duct cells of the pancreas of mice and rats. Eur J Morphol. **39**:277-283.

5. Fuchs JL, Schwark HD 2004 Neuronal primary cilia: a review. Cell Biol Int. **28**:111-118.

6. Whitfield JF 2004 The neuronal primary cilium--an extrasynaptic signaling device. Cell Signal. **16**:763-767.

7. Wandel A, Steigleder GK, Bodeux E 1984 [Primary cilia in cells of the epidermis and dermis]. Z Hautkr. **59**:382, 389-392.

8. Rupik W 2013 Ultrastructural studies of cilia formation during thyroid gland differentiation in grass snake embryos. Micron. **44**:228-237.

9. Klinck GH, Oertel JE, Winship T 1970 Ultrastructure of normal human thyroid. Lab Invest. **22**:2-22.

10. Sobrinho-Simoes M, Johannessen JV 1981 Scanning electron microscopy of the normal human thyroid. J Submicrosc Cytol. **13**:209-222.

11. Martin A, Hedinger C, Haberlin-Jakob M, Walt H 1988 Structure and motility of primary cilia in the follicular epithelium of the human thyroid. Virchows Arch B Cell Pathol Incl Mol Pathol. **55**:159-166.

12. Utrilla JC, Gordillo-Martinez F, Gomez-Pascual A, et al. 2015 Comparative study of the primary cilia in thyrocytes of adult mammals. J Anat. **227**:550-560.

13. Wheatley DN 2018 The primary cilium - once a "rudimentary" organelle that is now a ubiquitous sensory cellular structure involved in many pathological disorders. J Cell Commun Signal. **12**:211-216.

14. Wheatley DN 2005 Landmarks in the first hundred years of primary (9+0) cilium research. Cell Biol Int. **29**:333-339.

15. Wheatley DN 2010 Another decade of advances in research on primary cilia, porosomes and neosis: some passing thoughts at 70. Cell Biol Int. **34**:335-337.

16. Falk N, Losl M, Schroder N, Giessl A 2015 Specialized Cilia in Mammalian Sensory Systems. Cells. **4**:500-519.

17. Ishikawa H, Thompson J, Yates JR, 3rd, Marshall WF 2012 Proteomic analysis of mammalian primary cilia. Curr Biol. **22**:414-419.

18. Ishikawa H, Marshall WF 2011 Ciliogenesis: building the cell's antenna. Nat Rev Mol Cell Biol. **12**:222-234.

19. Wheway G, Nazlamova L, Hancock JT 2018 Signaling through the Primary Cilium. Front Cell Dev Biol. **6**:8.

20. Luo N, Conwell MD, Chen X, et al. 2014 Primary cilia signaling mediates intraocular pressure sensation. Proc Natl Acad Sci U S A. **111**:12871-12876.

21. Hildebrandt F, Benzing T, Katsanis N 2011 Ciliopathies. N Engl J Med. **364**:1533-1543.

22. Pugacheva EN, Jablonski SA, Hartman TR, et al. 2007 HEF1-dependent Aurora A activation induces disassembly of the primary cilium. Cell. **129**:1351-1363.

23. D'Angelo A, Franco B 2009 The dynamic cilium in human diseases. Pathogenetics. **2**:3.

24. Fan S, Hurd TW, Liu CJ, et al. 2004 Polarity proteins control ciliogenesis via kinesin motor interactions. Curr Biol. **14**:1451-1461.

25. Wang Q, Margolis B 2007 Apical junctional complexes and cell polarity. Kidney Int. **72**:1448-1458.

26. Lee J, Yi S, Kang YE, et al. 2016 Defective ciliogenesis in thyroid hurthle cell tumors is associated with increased autophagy. Oncotarget. **7**:79117-79130.

27. Gerard AC, Xhenseval V, Colin IM, et al. 2000 Evidence for co-ordinated changes between vascular endothelial growth factor and nitric oxide synthase III immunoreactivity, the functional status of the thyroid follicles, and the microvascular bed during chronic stimulation by low iodine and propylthiouracyl in old mice. Eur J Endocrinol. **142**:651-660.

28. Gerard AC, Many MC, Daumerie C, et al. 2002 Structural changes in the angiofollicular units between active and hypofunctioning follicles align with differences in the epithelial expression of newly discovered proteins involved in iodine transport and organification. J Clin Endocrinol Metab. **87**:1291-1299.

29. Gerard AC, Denef JF, Many MC, et al. 2003 Relationships between cell division, expression of growth factors and microcirculation in the thyroids of Tg-A2aR transgenic mice and patients with Graves' disease. J Endocrinol. **177**:269-277.

30. Colin I, Gerard AC 2010 The thyroid angiofollicular units, a biological model of functional and morphological integration. Bull Mem Acad R Med Belg. **165**:218-228; discussion 228-230.

31. Faggiano A, Coulot J, Bellon N, et al. 2004 Age-dependent variation of follicular size and expression of iodine transporters in human thyroid tissue. J Nucl Med. **45**:232-237.

32. Mizukami Y, Michigishi T, Nonomura A, et al. 1992 Histologic changes in Graves' thyroid gland after 131I therapy for hyperthyroidism. Acta Pathol Jpn. **42**:419-426.

33. Friedman NB, Catz B 1996 The reactions of euthyroid and hyperthyroid glands to radioactive iodine. Arch Pathol Lab Med. **120**:660-661.

34. Studer H, Ramelli F 1982 Simple goiter and its variants: euthyroid and hyperthyroid multinodular goiters. Endocr Rev. **3**:40-61.

35. Peter HJ, Studer H, Forster R, Gerber H 1982 The pathogenesis of "hot" and "cold" follicles in multinodular goiters. J Clin Endocrinol Metab. **55**:941-946.

36. Ramelli F, Studer H, Bruggisser D 1982 Pathogenesis of thyroid nodules in multinodular goiter. Am J Pathol. **109**:215-223.

37. Nesland JM, Sobrinho-Simoes M, Johannessen JV 1987 Scanning electron microscopy of the human thyroid gland and its disorders. Scanning Microsc. **1**:1797-1810.

38. Song Y, Driessens N, Costa M, et al. 2007 Roles of hydrogen peroxide in thyroid physiology and disease. J Clin Endocrinol Metab. **92**:3764-3773.

39. Ohye H, Sugawara M 2010 Dual oxidase, hydrogen peroxide and thyroid diseases. Exp Biol Med (Maywood). **235**:424-433.

40. Denef JF, Many MC, van den Hove MF 1996 Iodine-induced thyroid inhibition and cell necrosis: two consequences of the same free-radical mediated mechanism? Mol Cell Endocrinol. **121**:101-103.

41. Poncin S, Van Eeckoudt S, Humblet K, et al. 2010 Oxidative stress: a required condition for thyroid cell proliferation. Am J Pathol. **176**:1355-1363.

42. Colin IM, Denef JF, Lengele B, et al. 2013 Recent insights into the cell biology of thyroid angiofollicular units. Endocr Rev. **34**:209-238.

43. Paschke R 2011 Molecular pathogenesis of nodular goiter. Langenbecks Arch Surg. **396**:1127-1136.

44. Paschke R 2011 Nodulogenesis and goitrogenesis. Ann Endocrinol (Paris). **72**:117-119.

45. Berndorfer U, Wilms H, Herzog V 1996 Multimerization of thyroglobulin (TG) during extracellular storage: isolation of highly cross-linked TG from human thyroids. J Clin Endocrinol Metab. **81**:1918-1926.

46. Herzog V 1992 Regulation of the cellular transport and compactation of thyroglobulin. Exp Clin Endocrinol. **100**:12-13.

47. Herzog V, Berndorfer U, Saber Y 1992 Isolation of insoluble secretory product from bovine thyroid: extracellular storage of thyroglobulin in covalently cross-linked form. J Cell Biol. **118**:1071-1083.

48. Gerard AC, Denef JF, Colin IM, van den Hove MF 2004 Evidence for processing of compact insoluble thyroglobulin globules in relation with

follicular cell functional activity in the human and the mouse thyroid. Eur J Endocrinol. **150**:73-80.

49. Hassounah NB, Nagle R, Saboda K, et al. 2013 Primary cilia are lost in preinvasive and invasive prostate cancer. PLoS One. **8**:e68521.

50. Ergin AB, Saralaya S, Olansky L 2014 Incidental papillary thyroid carcinoma: clinical characteristics and prognostic factors among patients with Graves' disease and euthyroid goiter, Cleveland Clinic experience. Am J Otolaryngol. **35**:784-790.

51. Lee IS, Hsieh AT, Lee TW, et al. 2017 The Association of Thyrotropin and Autoimmune Thyroid Disease in Developing Papillary Thyroid Cancer. Int J Endocrinol. **2017**:5940367.

Table 1.- Baseline characteristics of the patients.

Pathological diagnosis	Age (Mean years old)	Gender	Thyroid status	Anti-TSR-R antibody level	Treatment	Response to treatment
Normal Thyroid	51,2 (42-69)	4 female 1 male	5 euthyroid	ND	TR-X	ND
Nodular Hyperplasia	52,5 (40-84)	9 female 1 male	8 euthyroid 1 hypothyroid 1 hyperthyroid	ND	TR-X	ND
Grave's Disease	45,7 (20-66)	8 female 2 male	10 hyperthyroid	10 high	10 Carbimazole	3 ND 3 Positive 4 Negative

ND, Non determined/ No Data; TR-X, total thyroidectomy.

FIGURE LEGENDS

Fig. 1.- Typical morphological aspects of thyroid follicles in normal thyroid glands (A), nodular hyperplasia (B) and Grave's disease (C) with Haematoxylin-eosin. In NT, although follicles of different sizes appear, their appearance is similar (A). In NH, more differences among follicles can be observed (B1). In GD, the heterogeneity among follicles increases considerably, showing areas with small and medium-sized follicles (C1), large follicles (C2), lymphocytic infiltrate (C3), hyperfunctioning follicles (C4), papillary follicles (C5) and, finally, follicles suffering apoptosis (C6). Scale bars, 25 μm.

Fig. 2.- Distribution of PC in normal thyroid glands using double immunofluorescence (E-cadherin, green; acetylated α-tubulin, red; nuclear counterstaining with DAPI, blue). Thyroid follicles exhibit numerous and easily recognizable PC oriented towards the colloid. Virtually every follicular cell displays at least one cilium (A-C), although the presence of two PC emerging in close proximity is not uncommon (D). In a tangential section of follicular epithelium, PC located in the center of the apical cell surfaces can be clearly seen (E). Scale bars, 25 μm.

Fig. 3.- Distribution of PC in nodular thyroid hyperplasia using double immunofluorescence (E-cadherin, green; acetylated α-tubulin, red; nuclear counterstaining with DAPI, blue). PC are observed in small follicles (A), medium-sized follicles (B), large follicles (C), and Sanderson's polsters epithelium (D). However, likely as a consequence of their small length, PC are only recognizable in part of the thyrocytes. Scale bars, 25 μm.

Fig. 4.- Distribution of PC in Grave's disease using double immunofluorescence (E-cadherin, green; acetylated α-tubulin, red; nuclear counterstaining with DAPI, blue). PC are reasonably identified in small follicles (A), medium-sized follicles (B), large follicles (C), follicles close to lymphocytic infiltrate (D), and in papillary follicles (E). However, hyperfunctioning follicles practically lack PC (F). Scale bars, 25 μm.

Fig. 5.- Percentage of ciliated follicular cells in the different patterns of thyroid follicles in normal thyroid (A), nodular hyperplasia (B), and Grave's disease (C). There are not statistically significant differences in the frequency of ciliated cells among different types of thyroid follicles in each group, with the exception of hyperfunctioning follicles in GD, which are the follicles where the fewest number of PC are detected. The results are expressed as mean ± SD. Data were compared using ANOVA one-way multiple comparison procedures (Dunn's method).***, P< 0.001

Fig. 6.- Comparison of the percentage of ciliated follicular cells among normal thyroid, nodular hyperplasia and Grave's disease. The frequency of ciliated thyrocytes is higher in normal thyroid, followed by NH and then GD. The comparisons among groups are significant. The results are presented as percentage of ciliated follicular cells, and expressed as mean ± SD. Data were compared using ANOVA one-way multiple comparison vs. control. ***, P< 0.001.

Fig. 7.- Comparison of percentages of ciliated follicular cells in "normal round-shaped follicles" of Grave's disease patients with different signs of thyroid activity. Primary cilia frequency in normal areas was significantly lower in patients who exhibited remaining hyperactive follicle foci, high T_4 serum levels or both, compared to those patients who showed no signs of hyperactivity after treatment. ***, P< 0.001.

Fig. 8.- Quantitative changes in the PC length among normal thyroid, nodular hyperplasia and Grave's disease. Normal thyrocytes show the longest PC of all groups, followed by thyrocytes in GD and, finally, thyrocytes from NH, which exhibit the shortest PC. The differences among groups were statistically significant. The results are expressed as mean ± SD. ***, P< 0.001.

Fig. 9.- Comparison of ciliary lengths of "normal round-shaped follicles" in Grave's disease patients with different signs of thyroid activity. Primary cilia length in normal areas was significantly shorter in patients who exhibited remaining hyperactive follicle foci, high T_4 serum levels or both, compared to

those patients who showed no signs of hyperactivity after treatment. ***, P< 0.001.

Fig. 10. Ultrastructure of normal thyroid gland (A), nodular hyperplasia (B), and Grave's disease (C) by TEM. In NT, a typical PC emerging perpendicularly from the apical surface of the thyrocyte into the colloid can be observed (A1). On higher magnification, the basal body and microtubular doublets within the ciliary shaft are displayed (A2). In NH, a much shorter PC is found emerging from the apex into the lumen of a flat follicular cell (B1, B2). In GD, a considerable heterogeneity among follicles can be observed, with papillary follicles (C1), very small follicles (C2), hyperfunctioning follicles exhibiting numerous microvilli (C3), lymphocytes emigrating through the follicular epithelium (C4), dome-shaped follicular cells (C5), tall thyrocytes with abundant lipofucsin and microvilli (C7), and, finally, scarce thyrocytes exhibiting PC (C7-8).

Fig. 11. Histological aspects of normal thyroid gland (A), nodular hyperplasia (B), and Grave's disease (C) by SEM. In NT, average normal-sized follicles can be observed (A1), with every thyrocyte exhibiting a PC emerging from the apical surface to the lumen (A2, A3). On higher magnification, numerous microvilli are seen on the apical cell surface (A2). When a lateral focus of the epithelium is obtained (A3), a pronounced convexity of the cellular apex and PC of considerable length are observed (A3). In NH, very large thyroid follicles are seen (B1), exhibiting a polyhedral epithelium with either smooth or rough apical cell surfaces (B2). At higher magnification, a PC and variable amounts of microvilli can be observed in different thyrocytes (B3). In GD, follicles bearing papillae are observed (C1), in which, at higher amplification, dome-shaped cells are distinguished (C2). The follicular epithelium can adopt different aspects, including the presence of dome-shaped cells with numerous microvilli and short PC (C3, C4).

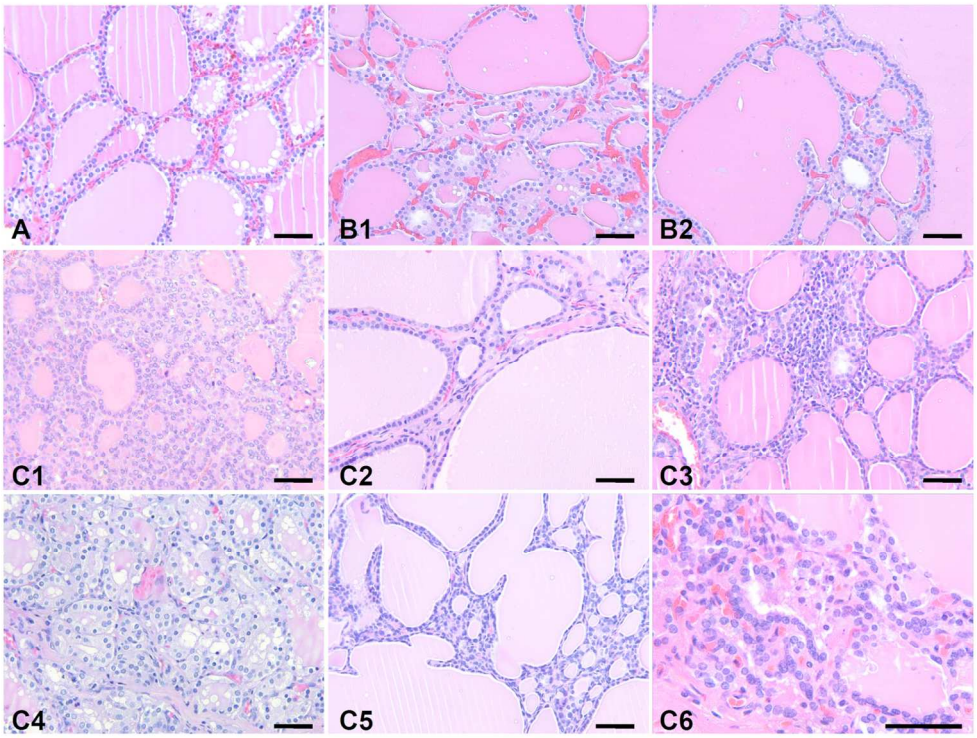

Fig. 1.- Typical morphological aspects of thyroid follicles in normal thyroid glands (A), nodular hyperplasia (B) and Grave's disease (C) with Haematoxylin-eosin. In NT, although follicles of different sizes appear, their appearance is similar (A). In NH, more differences among follicles can be observed (B1). In GD, the heterogeneity among follicles increases considerably, showing areas with small and medium-sized follicles (C1), large follicles (C2), lymphocytic infiltrate (C3), hyperfunctioning follicles (C4), papillary follicles (C5) and, finally, follicles suffering apoptosis (C6). Scale bars, 25 μm.

160x121mm (300 x 300 DPI)

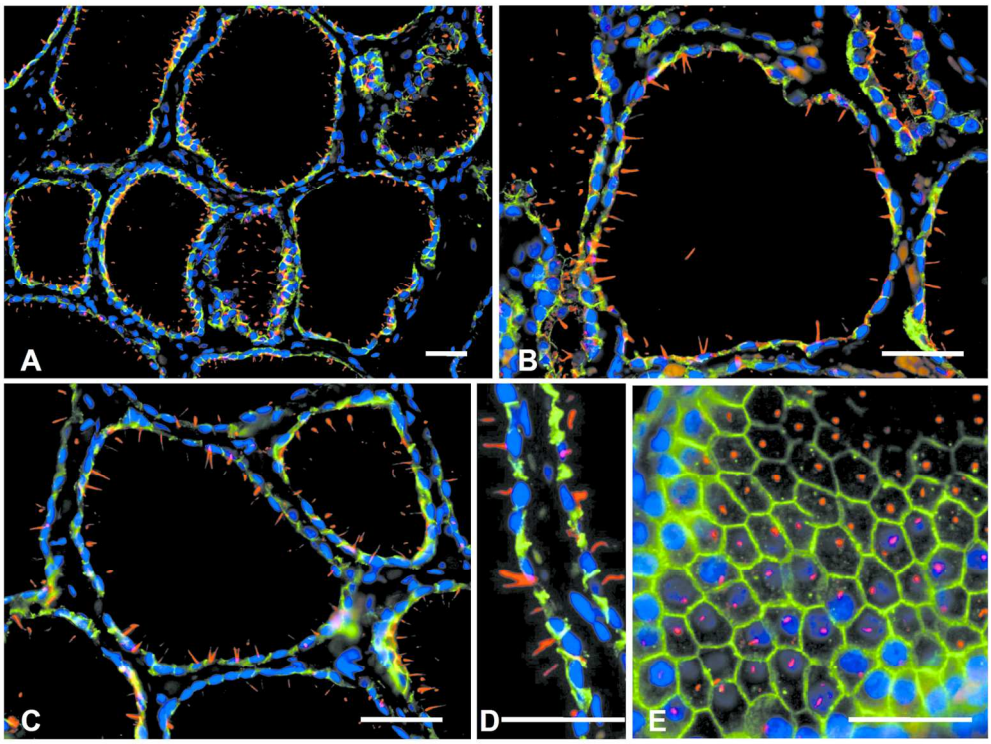

Fig. 2.- Distribution of PC in normal thyroid glands using double immunofluorescence (E-cadherin, green; acetylated α-tubulin, red; nuclear counterstaining with DAPI, blue). Thyroid follicles exhibit numerous and easily recognizable PC oriented towards the colloid. Virtually every follicular cell displays at least one cilium (A-C), although the presence of two PC emerging in close proximity is not uncommon (D). In a tangential section of follicular epithelium, PC located in the center of the apical cell surfaces can be clearly seen (E). Scale bars, 25 μm.

160x121mm (300 x 300 DPI)

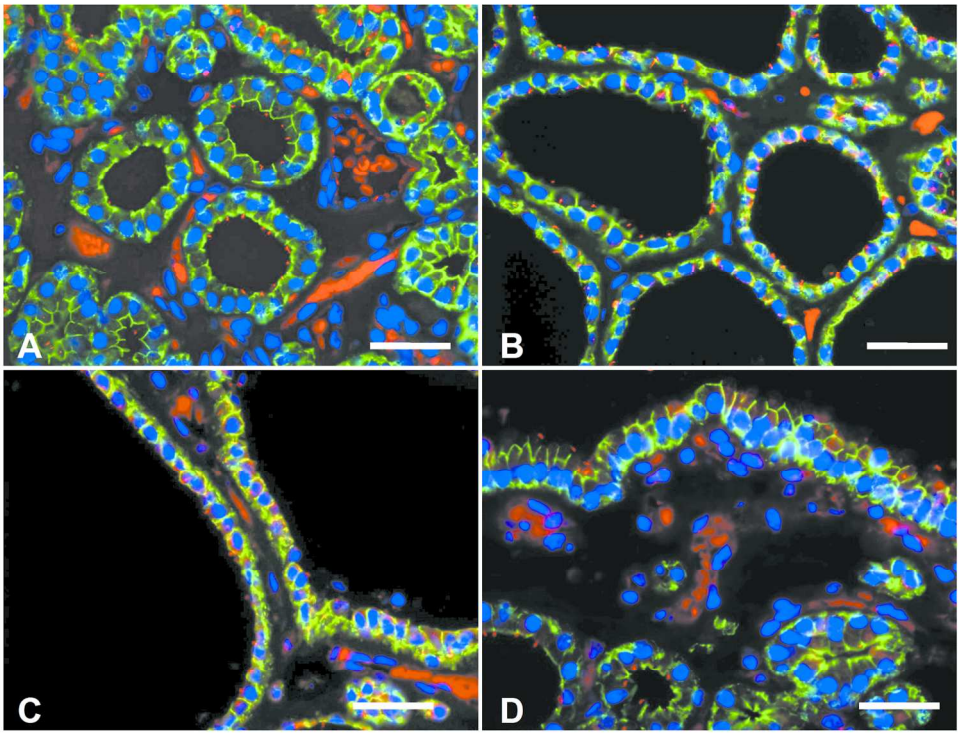

Fig. 3.- Distribution of PC in nodular thyroid hyperplasia using double immunofluorescence (E-cadherin, green; acetylated α-tubulin, red; nuclear counterstaining with DAPI, blue). PC are observed in small follicles (A), medium-sized follicles (B), large follicles (C), and Sanderson's polsters epithelium (D). However, likely as a consequence of their small length, PC are only recognizable in part of the thyrocytes. Scale bars, 25 μm.

160x127mm (300 x 300 DPI)

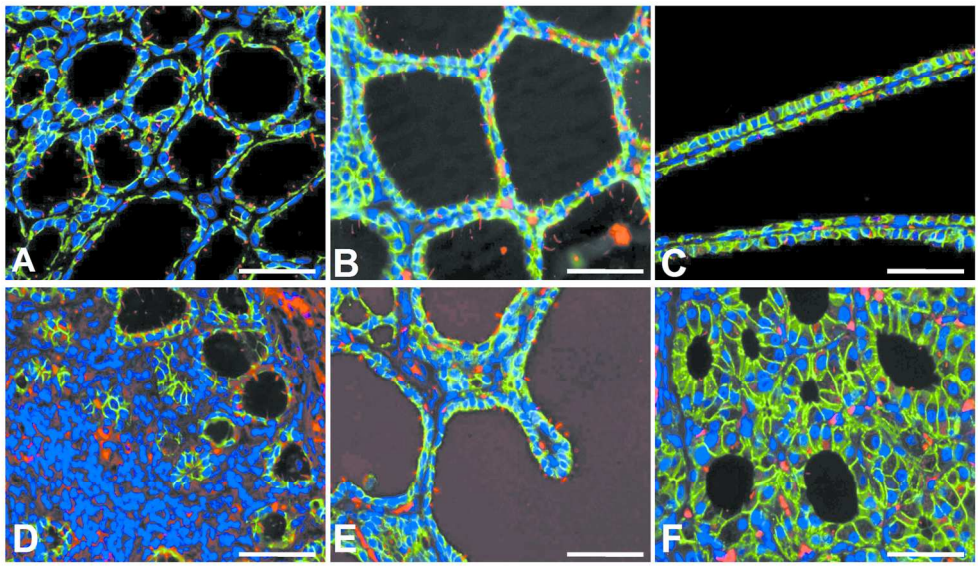

Fig. 4.- Distribution of PC in Grave's disease using double immunofluorescence (E-cadherin, green; acetylated α-tubulin, red; nuclear counterstaining with DAPI, blue). PC are reasonably identified in small follicles (A), medium-sized follicles (B), large follicles (C), follicles close to lymphocytic infiltrate (D), and in papillary follicles (E). However, hyperfunctioning follicles practically lack PC (F). Scale bars, 25 μm.

160x97mm (300 x 300 DPI)

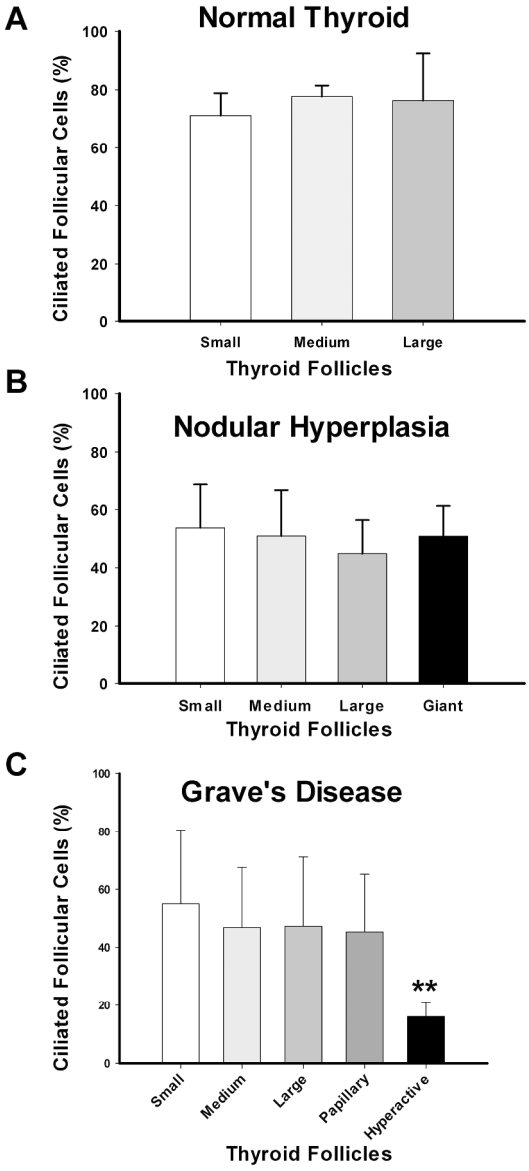

Fig. 5.- Percentage of ciliated follicular cells in the different patterns of thyroid follicles in normal thyroid (A), nodular hyperplasia (B), and Grave's disease (C). There are not statistically significant differences in the frequency of ciliated cells among different types of thyroid follicles in each group, with the exception of hyperfunctioning follicles in GD, which are the follicles where the fewest number of PC are detected. The results are expressed as mean ± SD. Data were compared using ANOVA one-way multiple comparison procedures (Dunn's method).***, P< 0.001

157x310mm (600 x 600 DPI)

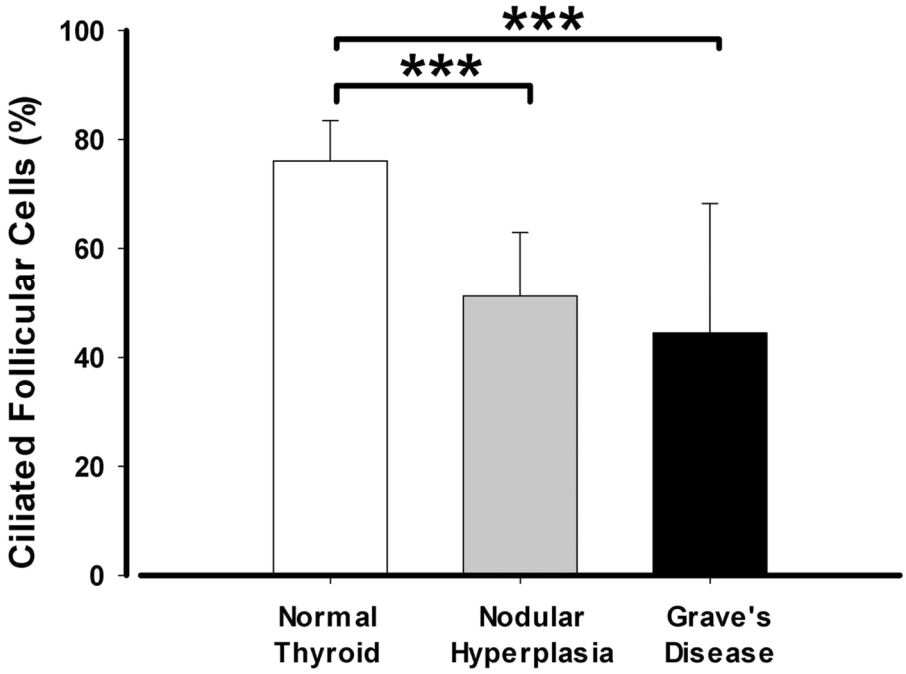

Fig. 6.- Comparison of the percentage of ciliated follicular cells among normal thyroid, nodular hyperplasia and Grave's disease. The frequency of ciliated thyrocytes is higher in normal thyroid, followed by NH and then GD. The comparisons among groups are significant. The results are presented as percentage of ciliated follicular cells, and expressed as mean ± SD. Data were compared using ANOVA one-way multiple comparison vs. control. ***, P< 0.001.

59x43mm (600 x 600 DPI)

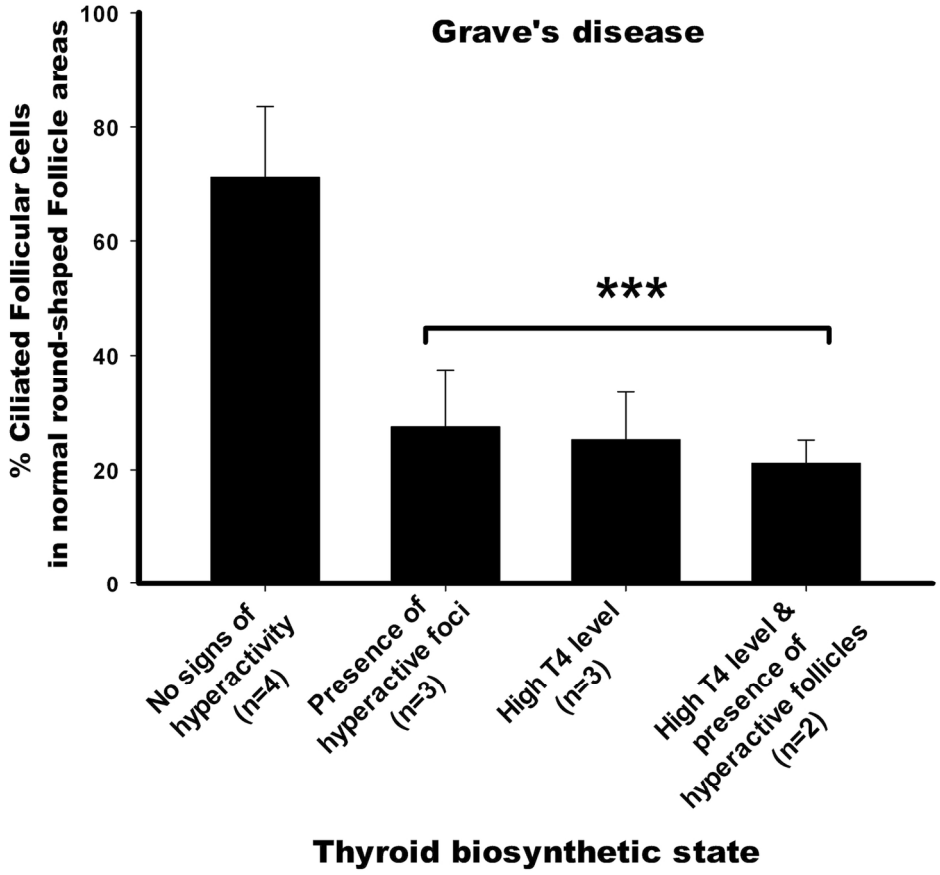

Fig. 7.- Comparison of percentages of ciliated follicular cells in "normal round-shaped follicles" of Grave's disease patients with different signs of thyroid activity. Primary cilia frequency in normal areas was significantly lower in patients who exhibited remaining hyperactive follicle foci, high T4 serum levels or both, compared to those patients who showed no signs of hyperactivity after treatment. ***, P< 0.001.

73x67mm (600 x 600 DPI)

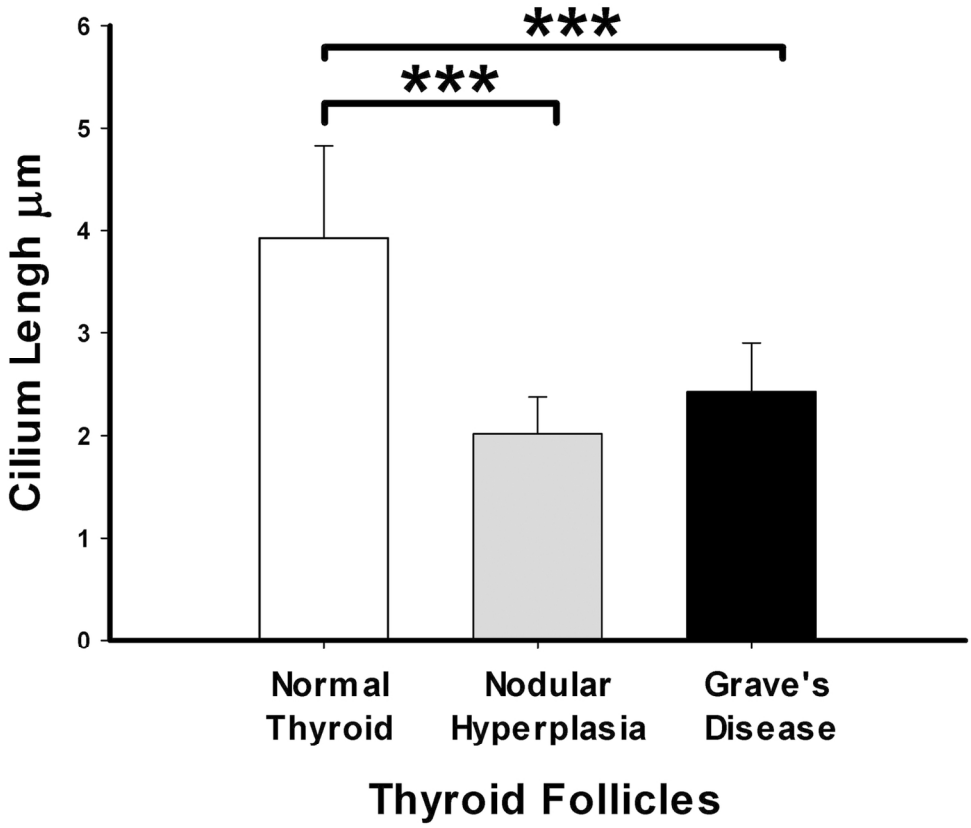

Fig. 8.- Quantitative changes in the PC length among normal thyroid, nodular hyperplasia and Grave's disease. Normal thyrocytes show the longest PC of all groups, followed by thyrocytes in GD and, finally, thyrocytes from NH, which exhibit the shortest PC. The differences among groups were statistically significant. The results are expressed as mean ± SD. ***, P< 0.001.

69x59mm (600 x 600 DPI)

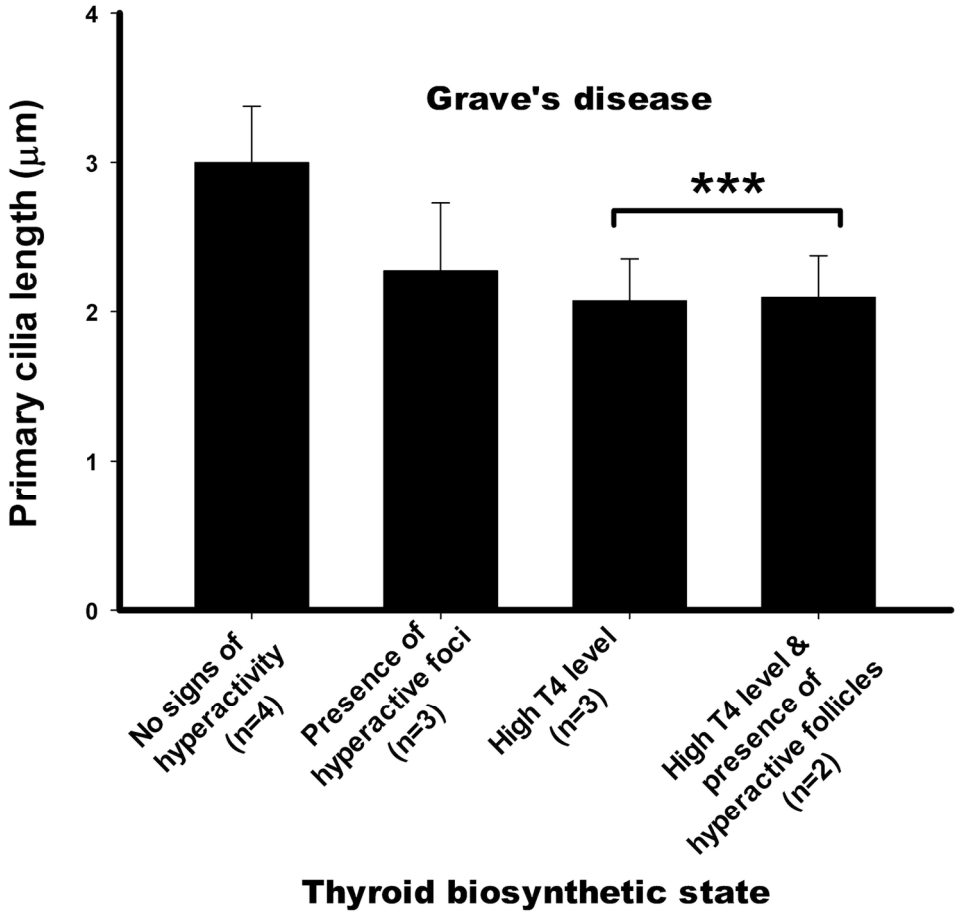

Fig. 9.- Comparison of ciliary lengths of "normal round-shaped follicles" in Grave's disease patients with different signs of thyroid activity. Primary cilia length in normal areas was significantly shorter in patients who exhibited remaining hyperactive follicle foci, high T4 serum levels or both, compared to those patients who showed no signs of hyperactivity after treatment. ***, P< 0.001.

75x71mm (600 x 600 DPI)

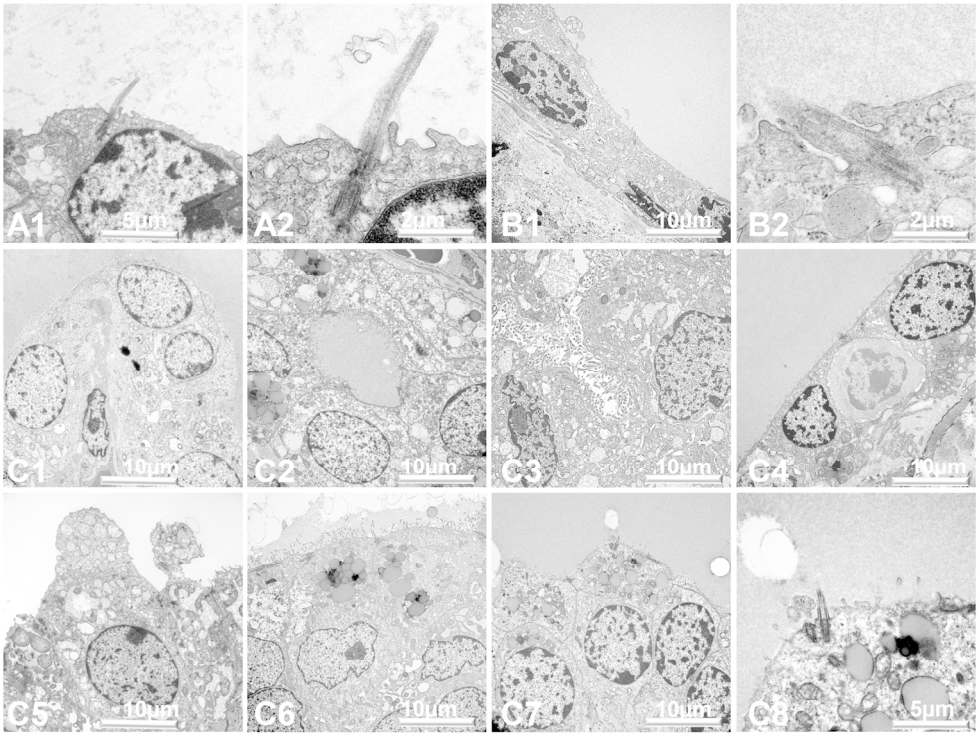

Fig. 10. Ultrastructure of normal thyroid gland (A), nodular hyperplasia (B), and Grave's disease (C) by TEM. In NT, a typical PC emerging perpendicularly from the apical surface of the thyrocyte into the colloid can be observed (A1). On higher magnification, the basal body and microtubular doublets within the ciliary shaft are displayed (A2). In NH, a much shorter PC is found emerging from the apex into the lumen of a flat follicular cell (B1, B2). In GD, a considerable heterogeneity among follicles can be observed, with papillary follicles (C1), very small follicles (C2), hyperfunctioning follicles exhibiting numerous microvilli (C3), lymphocytes emigrating through the follicular epithelium (C4), dome-shaped follicular cells (C5), tall thyrocytes with abundant lipofucsin and microvilli (C7), and, finally, scarce thyrocytes exhibiting PC (C7-8).

160x122mm (300 x 300 DPI)

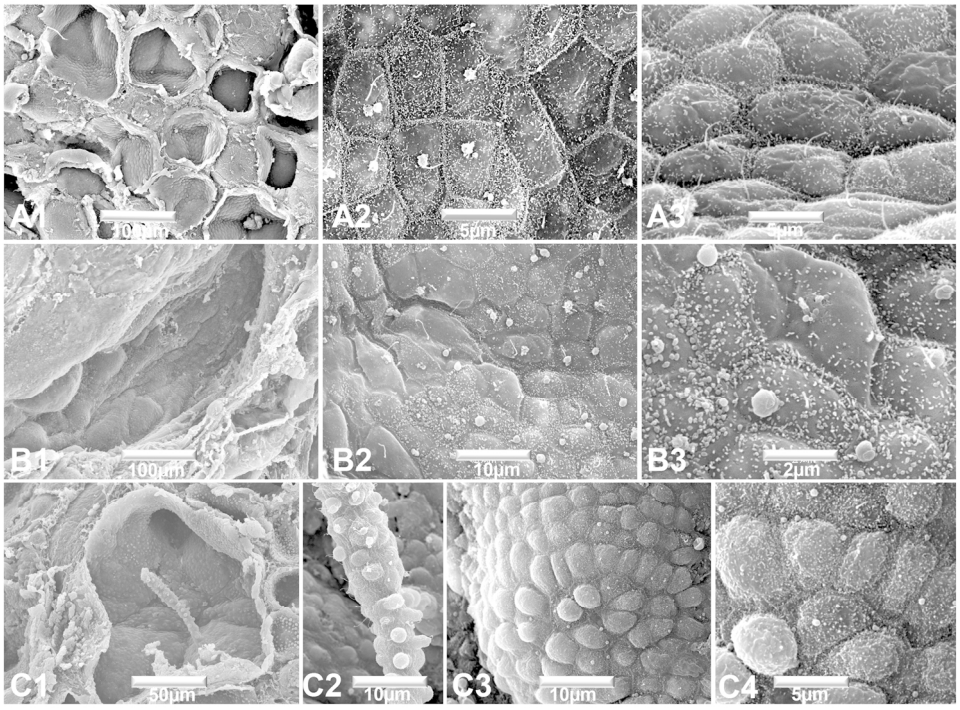

Fig. 11. Histological aspects of normal thyroid gland (A), nodular hyperplasia (B), and Grave's disease (C) by SEM. In NT, average normal-sized follicles can be observed (A1), with every thyrocyte exhibiting a PC emerging from the apical surface to the lumen (A2, A3). On higher magnification, numerous microvilli are seen on the apical cell surface (A2). When a lateral focus of the epithelium is obtained (A3), a pronounced convexity of the cellular apex and PC of considerable length are observed (A3). In NH, very large thyroid follicles are seen (B1), exhibiting a polyhedral epithelium with either smooth or rough apical cell surfaces (B2). At higher magnification, a PC and variable amounts of microvilli can be observed in different thyrocytes (B3). In GD, follicles bearing papillae are observed (C1), in which, at higher amplification, dome-shaped cells are distinguished (C2). The follicular epithelium can adopt different aspects, including the presence of dome-shaped cells with numerous microvilli and short PC (C3, C4).

160x117mm (300 x 300 DPI)